Dynamic corrosion of refractories by Na_2CO_3

Yu Xiang[1,a], Ying Zhao[1,b*], Lu Liu[1,c], Zongming Zheng[1], Changqing Dong[1]

[1] North China Electric Power University, Beijing, China

[a]xiang_yu1991@163.com, [b]zhaoying_1999@sohu.com, [c]381984879@qq.com

Keywords: dynamics, refractories, Na_2CO_3

Abstract. The corrosion of refractories by Na_2CO_3 at high temperature has become a severe issue. For a better understanding of corrosion mechanisms, this paper works out the kinetics mechanism of corrosion reaction including characteristic parameters and dynamics equation. The results provide the theoretical basis of sodium carbonate corrosion on refractories and give an evidence of the direction of corrosion resistance of refractories .

Introduction

Refractories are widely used in industries such as iron and steel,cement,and so on. However, there are severe corrosion in boilers. Therefore the scholars have studied in resistance of various refractory materials to corrosion, in order to solve the problem of corrosion.

Many researches show that refractories containing Cr_2O_3 have excellent performance in resistance to slag corrosion. Firstly, Cr_2O_3 has smaller solubility in the slag and could increase the viscosity of the molten slag, resulting in reducing chemical erosion of refractory,Secondly, increase of viscosity reduced the permeability and wettability of refractory materials and the formation of the metamorphic layer, thereby reducing flake refractory materials' structure. Refractory materials containing Cr2O3 have better performance among the basic refractory materials. But in waste incineration boiler alkali metal salts can cause severe corrosion in refractories, in addition, refractories were more prone to mechanical damage in high temperature, so that the service life of refractory material might be shorten and great hidden danger and economic losses might be happened.

Experimental

In order to have a better understanding of chromium refractory corrosion by Na_2CO_3, this paper studies the dynamic corrosion. Synchronous thermal analyzer (SDT) of the TA instrument company is provided for the experimental and its type is SDT-Q600. The samples will be analyzed with differential scanning calorimetry (DSC) and thermogravimetric analysis (TGA) at the same time. Its test temperature range from room temperature to 1500 ℃ and its measurable parameters include material internal change, heat flux, weight change. Raw materials are reacted at the ratio of 1:1 and the heating rate of 30℃ / min.

For isothermal reaction, the reaction rate is only a function of time under the certain reaction conditions. Thus, the study make the reaction rate of the reaction time under different reaction time in the dynamic equation of the form of linear according to the following table, resulting in the kinetic model and kinetic parameters.

Table 1 kinetic model

functions	mechanism	Integral form
G-B	Three dimensional diffusion, spherical symmetric, 3d, D4, deceleration α curve	$(1-2/3\alpha) - (1-\alpha)^{2/3}$
Jander	3 d, D3, reduction of α curve, n = 2	$[1-(1-\alpha)^{1/3}]^2$
Jander	Three dimensional diffusion, 3 d, n = 1/2	$[1-(1-\alpha)^{1/3}]^{1/2}$
Jander	The two-dimensional diffusion, 2 d, n = 1/2	$[1-(1-\alpha)^{1/2}]^{1/2}$
Avrami-Erofeev	Random nucleation and subsequent growth, A2, s-shaped α curve. N = 1/2, m = 2	$[-\ln(1-\alpha)]^{1/2}$
Avrami-Erofeev	Random nucleation and subsequent growth，A3, s-shaped α curve, n = 1/3, m = 3	$[-\ln(1-\alpha)]^{1/3}$
Avrami-Erofeev	Random nucleation and subsequent growth. N = 4	$[-\ln(1-\alpha)]^4$
Avrami-Erofeev	Random nucleation and subsequent growth, A4, s-shaped curve of α, n = 1/4, m = 4	$[-\ln(1-\alpha)]^{1/4}$
Avrami-Erofeev	Random nucleation and subsequent growth, n = 2	$[-\ln(1-\alpha)]^2$
Avrami-Erofeev	Random nucleation and subsequent growth, n = 3	$[-\ln(1-\alpha)]^3$
order reaction	n=3	$1-(1-\alpha)^3$
order reaction	n=2	$1-(1-\alpha)^2$
order reaction	n=4	$1-(1-\alpha)^4$
order reaction	n=1/4	$1-(1-\alpha)^{1/4}$
Mample Power	Phase boundary reaction (d), R1, n = 1	α
Mample Power	n=3/2	$\alpha^{3/2}$
Mample Power	n=1/2	$\alpha^{1/2}$
Mample Power	n=1/3	$\alpha^{1/3}$
Mample Power	n=1/4	$\alpha^{1/4}$

Results and Discussion
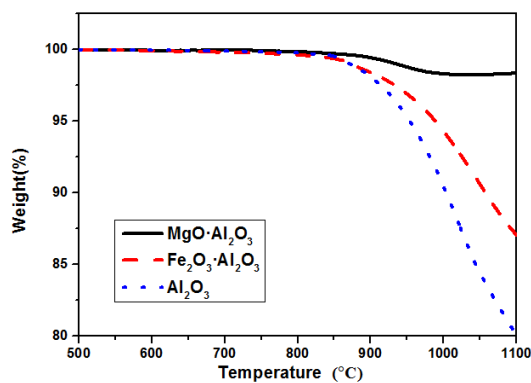
Fig.1 thermogravimetric curves of reactions of Al_2O_3-spinel with Na_2CO_3

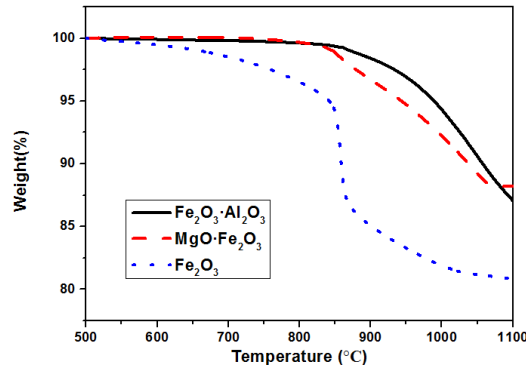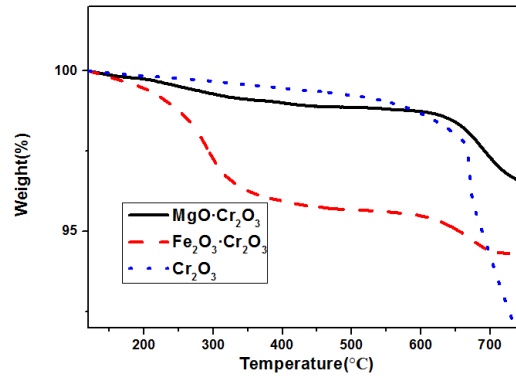Fig.2 thermogravimetric curves of reactions of Fe_2O_3-spinel with Na_2CO_3

Fig. 3 thermogravimetric curves of reactions of Cr_2O_3-spinel with Na_2CO_3

Fig.1 despicts that the reaction of Al_2O_3 with Na_2CO_3 at the heating rate of 30℃/min won't reach to reaction equilibrium when up to 1200℃. while Al_2O_3 began to react with Na_2CO_3 after 800 ℃ and the reaction speed up at 950 ℃. Magnesium aluminate spinel reactes with Na_2CO_3 at above 850℃ and when at 1200℃ the reaction is accelerated but not balance. The reaction of Hercynite with Na_2CO_3 began at around 800 ℃, accelerating rapidly with rising temperature. What's more, the reaction get the maximum reaction rate at 1048 ℃ and is not balanced when 1200℃.

Fig.2 shows the reaction of Fe_2O_3 with Na_2CO_3 is lower than the reaction of Na_2CO_3 with magnesium spinel reaction in temperature, speeding up at 700 ℃ and becoming a negative reaction between 850℃ to 860℃. The products of Magnesia spinel reacting with Na_2CO_3 under the condition of high temperature are magnesium and iron material. So thermogravimetric curve of weightlessness is caused by releasing CO_2 in the process of formating acid sodium and the weightlessness rate is related to reflecting the generated rate of sodium ferrate. magnesia spinel has the obvious reaction with Na_2CO_3 until around 800 ℃ and at about 1000 ℃ reach equilibrium.

Fig.3 illustrates the reaction of iron chromium spinel with Na_2CO_3 starts below 600℃ and balances out at around 750 ℃ at the heating rate of 30℃/min. Thermogravimetric curve shows that the reaction when 700 ℃ has been completed by more than 90%. reaction of Chrome oxide with Na_2CO_3 begin at about 600 ℃ and level off when 1000℃. Furthermore, reaction quickened at 680℃ and is more easy to take place than that of Fe_2O_3 with Na_2CO_3. Reaction of Magnesium chromium spinel with Na_2CO_3 speed when 600℃ and is basically reach equilibrium when 800 ℃.

According to the methods of studying kinetics under the condition of non-isothermal, reaction rates at different temperature are plugged into mechanism functions ($F(\alpha)$) in the table below and are resolved by linear regression method. Through the analysis of the linear correlation coefficient and the sum of squared residuals, there was a good linear relationship between $LnF(\alpha)/T^2$ and $1/T$ in process of Na_2CO_3 reacting with Fe_2O_3. Its process is in line with the Avrami - Erofeev model and its is random nucleation and growth. The integral form is $[-\ln(1-\alpha)]^4$. The formula of $F(\alpha)$ is in the following:

$$F(\alpha) = \int_0^\alpha \frac{d\alpha}{f(\alpha)} = \frac{ART^2}{\beta E}(1 - \frac{2RT}{E})e^{-\frac{E}{RT}}$$

$$\tag{1}$$

The dynamic results of corrosion reactions are in the following table.

Table 2: Dynamic analysis

Materials	E(kJ/mol)	A(min^{-1})	Kinetic Equations
Fe_2O_3	414.92	6.08×10^{43}	$d\alpha/dT=1.52\times10^{43}exp(-49.90\times1/T)(1-\alpha)[-ln(1-\alpha)]^{-3}$
Cr_2O_3	191.45	2.54×10^{15}	$d\alpha/dT=6.35\times10^{14}exp(-23.03\times1/T)(1-\alpha)[-ln(1-\alpha)]^{-3}$
Al_2O_3	849.75	4.40×10^{31}	$d\alpha/dT=1.10\times10^{31}exp(-102.20\times1/T)(1-\alpha)[-ln(1-\alpha)]^{-3}$
Iron chromium spinel	225.12	2.26×10^{10}	$d\alpha/dT=5.65\times10^{9}exp(-27.08\times1/T)(1-\alpha)[-ln(1-\alpha)]^{-3}$
Magnesium chromium spinel	460.15	1.13×10^{23}	$d\alpha/dT=2.83\times10^{22}exp(-55.35\times1/T)(1-\alpha)[-ln(1-\alpha)]^{-3}$
hercynite	672.81	3.97×10^{21}	$d\alpha/dT=9.93\times10^{20}exp(-80.91\times1/T)(1-\alpha)[-ln(1-\alpha)]^{-3}$
Iron magnesia spinel	905.75	5.22×10^{36}	$d\alpha/dT=1.31\times10^{36}exp(-108.93\times1/T)(1-\alpha)[-ln(1-\alpha)]^{-3}$
Magnesium aluminate spinel	1328.40	5.75×10^{53}	$d\alpha/dT=1.44\times10^{53}exp(-159.76\times1/T)(1-\alpha)[-ln(1-\alpha)]^{-3}$

Conclusion

Integral method is used to deal with thermogravimetric experiments data. Through linear regression method we know that the reactions of refractories with Na_2CO_3 are all in line with the Avrami - Erofeev model. In addition, the mechanism is random nucleation and growth and the integral form is $[-ln(1-\alpha)]4$. The characteristic parameters of reactions are obtained at the heating rate of 30℃/min. Reactions with Na_2CO_3 are sorted alphabetically by activation energy as follows: $Cr_2O_3 <$ iron chromium spinel $< Fe_2O_3 <$ magnesium, chromium spinel $<$ hercynite $< Al_2O_3 <$ alumina magnesia spinel $<$ magnesium aluminate spinel. Reaction kinetics equations are as follows:

$$d\alpha/dT=1/4Aexp(-E/RT)(1-\alpha)[-ln(1-\alpha)]^{-3} \tag{2}$$

Acknowledgement

References

[1]Yuejin Qian,Haijun Ren. The Application and Foreground of Refractories with Chromite[J]. Journal of Luoyang Technology College,2007,05:6-9.

[2]Li Zhang. Current Research Situation of Refractories for Waste Incinerator[J]. Industrial Furnace,2009,06:40-44.

[3]Mingzhen Zhao, Jin Liang. Study on refractory material and its development in China. Journal of the Graduates Sun Yat-Sen University:Natural Sciences and Medicine, 2012, 33(4): 17-24.

[4]Dianli Xu. Prospect of the development of refractory industry[J]. Seminar on the development strategy of the national refractory raw materials in the new situation,2014.

[5]Zuoshu Sun, Yan Zhang. Corrosion of Al_2O_3/CaO on high alumina refractories during the temperature cycle .Refractories & Lime, 2008 (4).

[6]Ming Xia, Experimental study on corrosion reaction of Mullite/Corundum refractories and alkaline sediments.Refractories & Lime,2014,04:55-61.

[7] Jian Hou, Jue Fang, Yanping Feng, Guosong Shi. Erosion of refractory by the ultra-high alkalinity slag produced in smelting ores from Guangxi [J]. Southern Metals,2009,02:28-30.

[8]Jinglin Liu. Application of MgO-C refractory materials with alkaline[J].Refractories& Lime,2008,03:16-20.

[9]Rong Quan. Erosion of sodium and potassium on refractory materials [J]. Refractories & Lime,2012,01:43-47.

[10]Pena P, Criado E, Bakali J J, et al. Dynamic corrosion of Al2O3–ZrO2–SiO2 and Cr2O3-containing refractories by molten frits. Part II: Microstructural study[J]. Journal of the European Ceramic Society, 2011, 31(5): 705-714.

[11]Prigent P, Bouchetou M L, Poirier J. Andalusite: An amazing refractory raw material with excellent corrosion resistance to sodium vapours[J]. Ceramics International, 2011, 37(7): 2287-2296.

[12]Stjernberg J, Lindblom B, Wikström J, et al. Microstructural characterization of alkali metal mediated high temperature reactions in mullite based refractories[J]. Ceramics international, 2010, 36(2): 733-740.

[13]R. Farris, J. Allen, Aluminous refractories—alkali reactions, Iron and Steel Engineering 50 (2) (1973) 67–74.

[14]Yong Xu. Study of reaction between Mullite/Corundum refractories and alkaline sediments . Refractories & Lime, 2013, 5: 013.

[15]Bläsing M, Schaafhausen S, Müller M. Investigation of alkali induced corrosion of SiC filter candles at high temperature, in gasification environment[J]. Journal of the European Ceramic Society, 2014, 34(4): 1041-1044.

[16]Prigent P, Bouchetou M L, Poirier J, et al. Corrosion of oxide bonded silicon carbide refractories by molten salts in solid waste-to-energy facilities[J]. Ceramics International, 2012, 38(7): 5643-5649.